"EVALUATION OF DIFFERENT CYCLING POSITIONS WITH HELP OF CFD TO ENHANCE PERFORMANCE OF PROFESSIONAL CYCLIST"

[1]ABHINAV D. SARDAR
Research Scholar, M.E. Thermal Engineering, Prof. Ram Meghe Institute of Technology & Research Badnera, Amravati, India
abhinavsardar05@gmail.com

[2]PROF. AKSHAY GOHAD
VYWS Polytechnic Badnera, Amaravti, India
akshaygohad02@gmail.com

[3]CHETAN G. JAWANJAL
Research Scholar, M.E. CAD-CAM Engineering, Prof. Ram Meghe Institute of Technology & Research Badnera, Amravati, India
jawanjal1990@gmail.com

[4]PIYUSH GULWADE
Research Scholar, M.E. CAD-CAM Engineering, Prof. Ram Meghe Institute of Technology & Research Badnera, Amravati, India

ABSTRACT**:** *When cycling on level ground at a speed greater than 14 m/s, aerodynamic drag is the most important resistive force. About 90% of the total mechanical power output is necessary to overcome it. Aerodynamic drag is mainly affected by the effective frontal area which is the product of the projected frontal area and the coefficient of drag. The effective frontal area represents the position of the cyclist on the bicycle and the aerodynamics of the cyclist-bicycle system in this position. In order to optimize performance, estimation of these parameters is necessary. The CFD is found to be a valuable tool to evaluate the drag of different cyclist positions and to investigate the influence of small adjustments in the cyclist's position which is the aim of our study. A strong advantage of CFD is that detailed flow field information is obtained, which cannot easily be obtained from wind-tunnel tests. This detailed information allows more insight in the causes of the drag force and provides better guidance for position improvements. describe and comment on the methods used during the last 30 years for the evaluation of the effective frontal area and the projected frontal area in cycling, in both laboratory and actual conditions. Finally, knowledge of these parameters can be useful in practice or to create theoretical models of cycling performance.*

Keywords: Aerodynamics drag, CFD, Coefficient of drag, Cyclist.

1. INTRODUCTION

The performance of cyclists is strongly affected by the resistance they experience, which consists of aerodynamic resistance or drag, rolling resistance, wheel-bearing and drive-train friction and road gradient. At high speeds (≈ 50 km/h), the majority of this resistance, about 90% or more, is caused by aerodynamic drag (Grappe et al., 1997; Kyle and Burke, 1984). Aerodynamic drag is a major concern of cycling research to enhance performance. During a cycling race (e.g. a time-trial), the time difference in performance between elite athletes can be small. The optimization of aerodynamic drag could be a determinant to enhance the cyclist's performance for the same mechanical power output. In order to minimize this resistance, it is important to know the determinant's parameters, how to evaluate them, and what the evolution of these parameters would be as a function of the position of the cyclist and his or her displacement velocity. The purpose of this review is to present the different assessment of aerodynamic drag and its most essential parameter, the effective frontal area, in order to enhance cycling performance.

2. CHARACTERISTIC OF THE AERODYNAMIC DRAG

The major performance parameter in cycling is the displacement velocity of both cyclist and bicycle (v, in m/s). At constant velocity, the ratio of the mechanical power output generated by the cyclist (P, in W) to the total resistive forces (RT, in N) is given by:

$$v = \frac{P}{R_T}$$

By definition, the power output is the quantity of energy output per unit time. At constant speed, the mechanical power output can be assumed to be the sum of the energy used to overcome the total resistive forces (De Groot et al., 1995; di Prampero, 2000). Since aerodynamic drag is about 90% of the total resistive forces at high speed (. 14 m/s), for a constant power output decreasing aerodynamic drag would result in an increase of the velocity of the cyclist-bicycle system. In all forms of human-powered locomotion on land, aerodynamic drag is directly proportional to the combined projected frontal area of

the cyclist and bicycle (Ap, in m2), the drag coefficient (CD, dimensionless), air density (r, in kg/m3) and the square of the velocity relative to the fluid (vf, in m/s). RD can be expressed by (e.g. di Prampero et al., 1979):

$$R_D = 0.5.A_P C_D \rho V_f^2$$

For a given velocity, aerodynamic drag is dependent on air density and the effective frontal area (ApCD, inm2). Air density is directly proportional to the barometric pressure of the fluid (PB, in mmHg) and inversely proportional to absolute temperature (T, in K) (di Prampero, 1986):

$$\rho = \rho_0 . \left(\frac{PB}{760}\right) . \left(\frac{273}{T}\right)$$

Where r0 ¼ 1.293 kg/m3, the air density at 760mmHg and 273 K. Air density is also affected by air humidity but this effect is very small and can be neglected (di Prampero, 2000). Moreover, at a given temperature, the barometric pressure of fluid decreases with the altitude above sea level (Table I). At a temperature of 273 K, the decrease in barometric pressure of the fluid with altitude (Alt, in km) can be described by (di Prampero, 2000):

Table I. Effect of air density on aerodynamic drag

Track	**Alt (km)**	**PB (mmHg)**	ρ^a **(kg/m^3)**	**RD^b (N)**
Street Road	0	760	1.20	29.8
Street Road	1.84	605	0.96	23.9
Street Road	2.25	575	0.91	22.6

Alt = Altitude; PB = Barometric Pressure; ρ = Air density; R_D =Aerodynamic drag; Ap =Projected frontal area; C_D =Coefficient of drag; vf = Velocity relative to the fluid.;

3. THE PROJECTED FRONTAL AREA

The projected frontal area represents the portion of a body which can be seen by an observer placed exactly in front of that body, i.e. the projected surface normal to the fluid displacement. Some authors assume that the projected frontal area is a constant fraction of the body surface area to establish mathematical descriptions of aerodynamic drag (e.g. Capelli et al., 1993). This assumption is helpful since the body surface area (ABSA, inm2) is easily estimated from the measurement of two anthropometric parameters, body height (hb, in cm) and body mass (mb, in kg) (Du Bois & Du Bois, 1916; Shuter & Aslani, 2000):

$$A_{BSA} = 0.00949.h_b^{0.655}.m_b^{0.441}$$

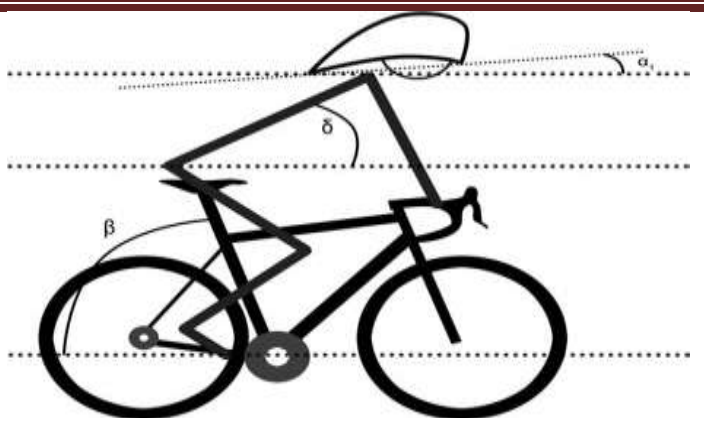

Fig(1): Seat tube angle (β),Trunck Angle(δ),Helmet angle(α)

However, the projected frontal area is not proportional to the body surface area because the ABSA/mb ratio tends to be smaller in larger cyclists. (Heil, 2001) reported that the assumption that the projected frontal area and body surface area are proportional is correct for cyclists with a body mass of between 60 and 80 kg. It is generally considered that the body surface area is proportional to m0:667 b , whereas the projected frontal area is proportional to m0:762 b (Heil, 2001). The projected frontal area also can be expressed with the position of the cyclist on the bicycle from the seat tube angle (b, in degree) and the trunk angle (d, in degree) relative to the horizontal (Figure 1). The trunk is represented by the body segment between the hip and shoulder. A goniometer was used to measure the trunk angle:

$$A_P = 0.11433.\beta^{0.172}.\partial^{0.096}.m_b^{0.762}$$

Nonetheless, Garcia-Lopez et al. (2008) observed a weak correlation between the trunk angle and the projected frontal area (r ¼ 0.42, p , 0.05). Finally, as logically expected, the results of the different studies show that the projected frontal area is dependent on body height and body mass, position on the bicycle, and equipment used (e.g. helmet, shape of the frame, clothes). Faria et al. (2005) reported a method to determine the projected frontal area in the aerodynamic position with aero-handlebars using body height and body mass:

$$A = 0.0293.h_b^{0.725}.m_b^{0.425} + 0.0604$$

Barelle et al. (2010) established two models to determine the projected frontal area in the aerodynamic position with aero-handlebars and a time-trial helmet, as a function of body height, body mass, length of the helmet (L, in m), and its inclination on the horizontal (a1, in degree) (Figure 1):

$$A_P = 0.107.h_b^{1.6858} + 0.329.(L.\sin\alpha_1)^2 - 0.137.(L\sin\alpha_1)$$
$$A_P = 0.045.h_b^{1.15}.m_b^{0.2794} + 0.329.(L.\sin\alpha_1)^2 - 0.137.(L\sin\alpha_1)$$

4. THE DRAG COEFFICIENT

The drag coefficient is used to model all the complex factors of shape, position, and air flow conditions relating to the cyclist. The drag coefficient is the ratio between aerodynamic drag and the product of dynamic pressure (q, in Pa) of moving air stream and the projected frontal area (Pugh, 1971):

$$C_D = \frac{R_D}{qA_P}$$

Where the dynamic pressure is equivalent to the kinetic energy per unit of volume of a moving solid body, and defined by the equation:

$$q = \frac{1}{2}.\rho.V_f^2$$

The drag coefficient is dependent on the Reynolds number. The Reynolds number is a dimensionless number that gives a measure of the ratio of inertial forces to viscous forces. Thus, the drag coefficient depends on the air velocity and the roughness of the surface. For a given position on the bicycle, the relationship between aerodynamic drag and velocity relative to the fluid is not linear.

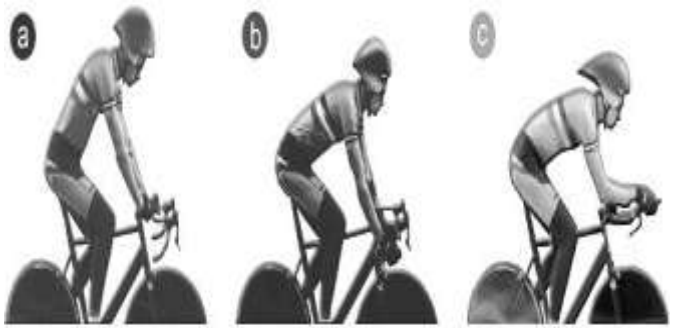

Fig (2): Different cycling positions: (a) upright (b) dropped, and (c) time trial.

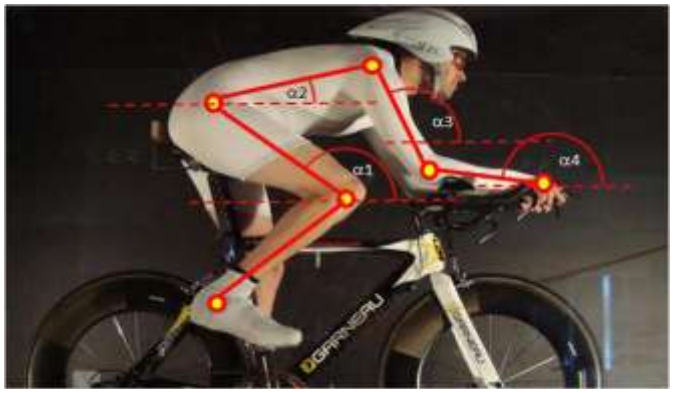

Fig (3): Angles of different cycling positions.

Table (2): Angles of different cycling positions.

Body segment (angle)	**Upright Position**	**Dropped Position**	**Time Trial Position**
Thigh	0^0-115^0	0^0-115^0	0^0-115^0
Trunk	45^0	30^0	0^0
Arm	115^0	105^0	105^0
Forearm	115^0	105^0	0^0

5. CFD (Computational Fluid Dynamics) Simulation

Three different cyclist positions were evaluated with Computational Fluid Dynamics (CFD) and to provide reliable data to evaluate the accuracy of the CFD simulations. Specific features of this study are: (1) Both steady Reynolds-averaged Navier-Stokes (RANS) and unsteady flow modelling, with more advanced turbulence modelling techniques (Large-Eddy Simulation - LES), were evaluated; (2) The boundary layer on the cyclist's surface was resolved entirely with Low-Reynolds number modelling, instead of modelling it with wall functions. The results show that the simulated and measured drag areas differed about 11% (RANS) and 7% (LES), which is considered to be a close agreement in CFD studies A strong advantage of CFD is that detailed flow field information is obtained, which cannot easily be obtained from wind-tunnel tests. This detailed information allows more insight in the causes of the drag force and provides better guidance for position improvements The aim of this study is to evaluate the use of CFD for the analysis of aerodynamic drag of different cycling positions and to examine and improve some CFD modelling studies for sport applications. Steady RANS and (unsteady) Large-Eddy Simulation (LES) turbulence modeling techniques are compared where the boundary layer on the cyclist's surface is resolved entirely, instead of being modeled by wall functions. For CFD evaluation purposes, wind-tunnel experiments on a full-scale cyclist were carried out for three cyclist positions. Apart from drag measurements, also surface pressure measurements on the cyclist's body were performed to allow evaluation of the predicted flow field of CFD to some extent.

The drag areas obtained by the wind-tunnel experiments, for the cyclist without bicycle setup CFD simulations with RANS and LES for the three cyclist positions. For all positions, the accuracy of LES is equal to or higher than RANS, which is probably due to a better prediction of the wake flow.

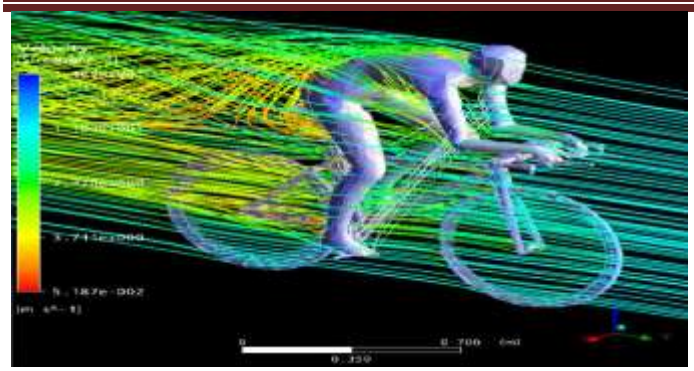

Fig (4): Wind Tunnel Test

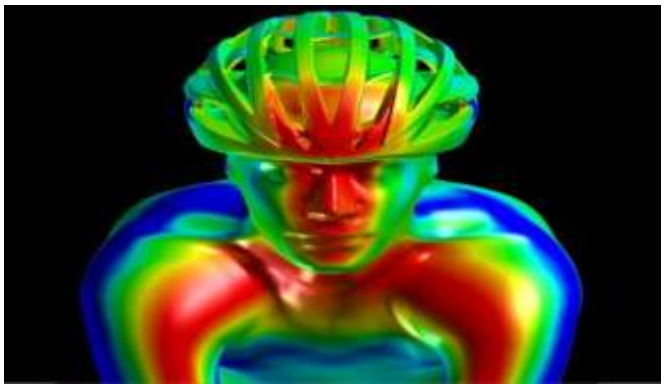

Fig(5):CFD Simulation Test

Fig (6): Effect of CFD Simulations Test on Front And Back Side of Cyclist.

The systematically higher drag areas found for CFD, compared to wind tunnel data, could be attributed to several reasons: (1) Only the cyclist is modelled in the CFD simulations and thereby the interference drag with the bicycle setup is not accounted for; (2) The CFD simulations are performed assuming a perfectly smooth cyclist surface, since surface roughness cannot be specified if LRNM is used to model the boundary layer. In the wind-tunnel experiment however, the cyclist's surface was not perfectly smooth due to the cyclist's clothing. As a result, the predicted skin-friction drag should be lower in the CFD simulations. Since it is only a small percentage of the total drag for bluff bodies, namely about 5% in this study (predicted by CFD simulations), the resulting decrease of the total drag will be limited and could even not be noticed: the total drag area obtained with CFD is actually higher than the wind-tunnel data. More important however is the fact that surface roughness could alter the locations where boundary-layer separation occurs on the cyclist's surface by which the flow field around the cyclist will change and therefore also the resulting from drag. Under appropriate conditions, a boundary layer could remain more attached on a rough surface (i.e. in the wind tunnel in this study) by which the wake zone and therefore also the total drag are reduced (Wilson, 2004). This could explain why the "smooth" cyclist of CFD exhibits a systematically higher drag area; (3) The surface details of the cyclist (e.g. eyes or nose) are smoothed out to some extent in the computational model; and (4) Even very sophisticated turbulence modelling techniques, like LES, still always "model" (i.e. approximate instead of solve) some parts of the turbulent flow, by which there will inherently be a difference with the actual flow conditions, 5 most likely in the wake of the cyclist. As argued above however, the discrepancies are not only related to turbulence modelling but also to simplifications to the computational model. In Figure 5 and 6, the CP coefficients obtained with the wind-tunnel experiments are compared to the results from the CFD simulations, for RANS and LES (time-averaged CP values), for the UP and TTP positions. The CP coefficient is defined as:

$$C_P = \frac{(P_{SURF} - P_{INL})}{\frac{\rho U^2}{2}}$$

where psurf is the static pressure on the cyclist's body and pinl is the static pressure at the inlet of the wind-tunnel test section. For the CFD simulations, pinl is the average pressure at the inlet of the computational domain. Note however that this inlet is not located at the same location as the inlet of the wind-tunnel test section, which is done to limit the size of the upstream part of the computational domain. As expected, an overpressure is found on the front side of the cyclist, leading to positive CP values, whereas in the wake of the cyclist, negative CP values are found. Note that the CP values, obtained in the wind tunnel, are reported for 20 m/s in Figure 5 and 6 since the relative accuracy of the CP values is higher at high wind speeds. The use of these CP values instead of those at 10 m/s can be justified since no significant Reynolds number effects were noticed. Since the location of the pressure sensors could not be determined exactly, the reported CFD data are actually the averaged pressures within a circular zone (radius 2.5 cm) on the surface of the cyclist. The uncertainty band for the CFD results is the standard deviation from this averaged value. For the uncertainty of the wind-tunnel data, the measurement error on the pressure plates (7 Pa) is used, which is larger than the standard deviation on CP for almost all points. The numbers of the sensors (see Figure 3), where the differences between wind-tunnel data and CFD are significant, are indicated in Figure 5 and 6. Note that a good agreement of CFD with wind-tunnel measurements implies that the data are all located near the solid line which is shown in the figures. The dotted lines represent 25% deviation from this solid line. A good to very good agreement is found for most pressure plates for both cyclist positions and for both RANS and LES, especially for the TTP position. Note that the points that show the largest discrepancies are those on the side of the cyclist (points 27-30). This is the

case for both cyclist positions. At these points, the CFD simulations predict too high negative pressure coefficients. This again could be a result from the difference in the location of the separation points, which is indicated by a larger under pressure for CFD, where boundary-layer separation seems to occur faster. Distinct outliers are also found at points 3, 4 and 8 for the UP position and at point 10 for the TTP position. Especially, the lower CP value for point 3 in the wind-tunnel experiment has an obvious cause, namely the fact that this point is in the wake of a part (slender beam) of the bicycle setup (Figure 2a). If the RANS and LES simulation results are compared, it is clear that LES provides a higher accuracy, both for drag and surface pressures. The much larger computational cost of LES compared to steady RANS, i.e. about one order of magnitude, and the additional temporal sensitivity analysis that is required however makes it much less attractive for practical calculations. Despite the (small) differences between CFD and wind-tunnel results, the main advantage of CFD is that detailed flow field information is obtained, which allows more insight into the causes of the drag force, e.g. the wake flow, and which provides better guidance for position improvements. Note however that it is difficult to obtain an "absolute" optimum rider positioning by means of wind-tunnel tests or CFD simulations since both optimization approaches will always differ to some extent from reality (see Section 2), which is dependent on the environmental conditions, the size of the group in which the cyclist is riding and his position with respect to the others, etc. Different "optimal" positions can therefore be found, depending on the specific conditions.

Fig (7): Physical Position of Cyclist (a) and (b).

Fig (8): Locations of the pressure plates on the cyclist's surface (30 plates in total).

Figure (9): Comparison between pressure coefficients of wind-tunnel tests ($C_{P,WT}$) and CFD simulations ($C_{P,CFD}$) (with uncertainty bands) for the upright position (UP): (a) RANS simulations; (b) LES simulations. The dotted lines represent 25% deviation from the solid line**.**

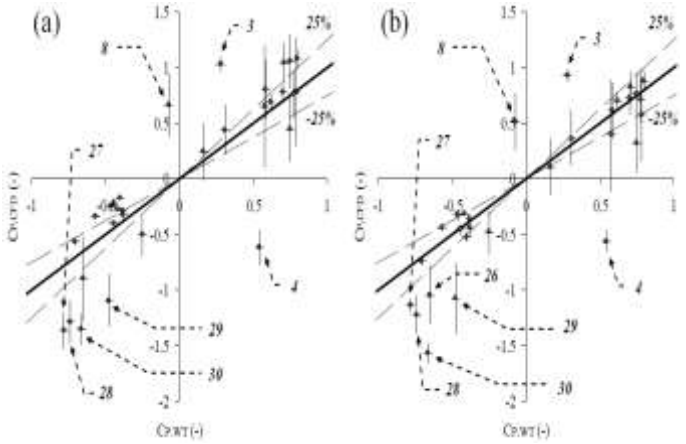

Figure (10): Comparison between pressure coefficients of wind-tunnel tests ($C_{P,WT}$) and CFD simulations ($C_{P,CFD}$) (with uncertainty bands) for the time-trail position (TTP): (a) RANS simulations; (b) LES simulations. The uncertainty band for $C_{P,CFD}$ is the standard deviation from the averaged value within a circular zone (radius 2.5 cm) on the surface of the cyclist. For the uncertainty of $C_{P,WT}$, the measurement error on the pressure plates (7 Pa) is used. The dotted lines represent 25% deviation from the solid line.

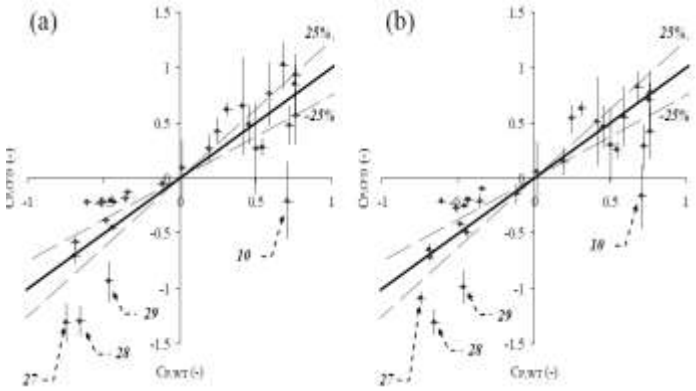

6. CONCLUSION

In this study, the drag areas obtained by wind-tunnel experiments showed good agreement with previous experiments. The CFD simulations predicted the drag areas with an accuracy of about 11% for RANS and about 7% for LES, which is considered to be a close agreement in CFD studies. A relatively good agreement was also obtained for the CP values, especially for the aerodynamic position and when using LES (for all positions). The CP measurements allowed for a more in depth comparison of RANS and LES than only the drag areas. The discrepancies between CFD and wind-tunnel data were not entirely related to limitations of the turbulence modelling itself but were also attributed to simplifications made in the

computational model. Regarding the turbulence modelling, LES is found to provide more accurate flow predictions than RANS, but the increased computational cost does not always justify this increased accuracy. This study has shown that CFD is a valuable alternative to evaluate the drag of different cyclist positions with sufficient accuracy and to investigate the influence of small adjustments in cyclist positions. Its main advantage is that detailed flow field information is obtained, which allows more insight in the causes of the drag force and provides better guidance for position improvements.

7. REFERENCES

[1]Grappe, F., Candau, R., Belli, A., & Rouillon, J. D. (1997). Aerodynamic drag in field cycling with special reference to the Obree's position. Ergonomics, 40, 1299 1311

[2] De Groot, G., Sargeant, A., & Geysel, J. (1995). Air friction and rolling resistance during cycling. Medicine and Science in Sports and Exercise, 27, 1090–1095.Retrieved from http://journals.lww.com/acsm-msse/Abstract/ 1995/07000/Air_friction_and_rolling_resistance_during_cycling .20.as

[3] di Prampero, P. E., Cortili, G., Mognoni, P., & Saibene, F. (1979). Equation of motion of a cyclist. Journal of Applied Physiology, 47, 201–206. Retrieved from http://jap.physiology.org/content/47/1/201.

[4] di Prampero, P. E. (1986). The energy cost of human locomotion on land and in water. International Journal of Sports and Medicine, 7, 55–72.

[5] di Prampero, P. E. (2000). Cycling on earth, in space and on the moon. European Journal Applied of Physiology, 82, 345–36

[6] Capelli, C., Rosa, G., Butti, F., Ferretti, G., & Veicsteinas, A. (1993). Energy cost and efficiency of riding aerodynamics bicycles. European Journal of Applied Physiology, 67, 144–149.

[7] Shuter, B., & Aslani, A. (2000). Body surface area: Du Bois and Du Bois revisited. European Journal of Applied Physiology, 82, 250–254.

[8] Heil, D. P. (2001). Body mass scaling of projected frontal area in competitive cyclists. European Journal of Applied Physiology, 85, 358–366.

[9] Garcia-Lopez, J., Rodriguez-Marroyo, J. A., Juneau, C.-E., Peleteiro, J., Cordova Martinez, A., & Villa, J. G. (2008). Reference values and improvement of aerodynamic drag in professional cyclists. Journal of Sports Sciences, 26, 277–286.

[10] Faria, E. W., Parker, D. L., & Faria, I. E. (2005). The science of cycling: Factors affecting performance – Part 2. Sports Medicine, 35, 313–337. Retrieved from http://adisonline.com/sportsmedicine/Abstract/2005/35040/The_ Science_of_Cycling__Factors_Affecting.3.aspx

[11] Barelle, C., Chabroux, V., & Favier, D. (2010). Modeling of the time trial cyclist projected frontal area incorporating anthropometric, postural and helmet characteristics. Sports Engineering, 12, 199–206.

[12] Pugh, L. G. C. E. (1971). The influence of wind resistance in running and walking and the mechanical efficiency of work against horizontal or vertical forces. Journal of Physiology, 213, 255–276. Retrieved from http://jp.physoc.org/content/213/2/255.

[13] Wilson, D.G., 2004. Bicycling Science. 3rd Ed. MIT Press, USA.